

Relationship between NaCl- and H₂O₂-Induced Cytosolic Ca²⁺ Increases in Response to Stress in *Arabidopsis*

Zhonghao Jiang^{1,2,3*}, Shan Zhu^{2*}, Rui Ye³, Yan Xue³, Amelia Chen³, Lizhe An¹, Zhen-Ming Pei^{2,3*}

1 The Key Laboratory of Cell Activities and Stress Adaptations, School of Life Science, Lanzhou University, Lanzhou, Gansu, China, **2** Center on Plant Environmental Sensing, Institute for Global Change, College of Life and Environmental Sciences, Hangzhou Normal University, Hangzhou, Zhejiang, China, **3** Department of Biology, Duke University, Durham, North Carolina, United States of America

Abstract

Salinity is among the environmental factors that affect plant growth and development and constrain agricultural productivity. Salinity stress triggers increases in cytosolic free Ca²⁺ concentration ([Ca²⁺]_i) via Ca²⁺ influx across the plasma membrane. Salinity stress, as well as other stresses, induces the production of reactive oxygen species (ROS). It is well established that ROS also triggers increases in [Ca²⁺]_i. However, the relationship and interaction between salinity stress-induced [Ca²⁺]_i increases and ROS-induced [Ca²⁺]_i increases remain poorly understood. Using an aequorin-based Ca²⁺ imaging assay we have analyzed [Ca²⁺]_i changes in response to NaCl and H₂O₂ treatments in *Arabidopsis thaliana*. We found that NaCl and H₂O₂ together induced larger increases in [Ca²⁺]_i in *Arabidopsis* seedlings than either NaCl or H₂O₂ alone, suggesting an additive effect on [Ca²⁺]_i increases. Following a pre-treatment with either NaCl or H₂O₂, the subsequent elevation of [Ca²⁺]_i in response to a second treatment with either NaCl or H₂O₂ was significantly reduced. Furthermore, the NaCl pre-treatment suppressed the elevation of [Ca²⁺]_i seen with a second NaCl treatment more than that seen with a second treatment of H₂O₂. A similar response was seen when the initial treatment was with H₂O₂; subsequent addition of H₂O₂ led to less of an increase in [Ca²⁺]_i than did addition of NaCl. These results imply that NaCl-gated Ca²⁺ channels and H₂O₂-gated Ca²⁺ channels may differ, and also suggest that NaCl- and H₂O₂-evoked [Ca²⁺]_i may reduce the potency of both NaCl and H₂O₂ in triggering [Ca²⁺]_i increases, highlighting a feedback mechanism. Alternatively, NaCl and H₂O₂ may activate the same Ca²⁺ permeable channel, which is expressed in different types of cells and/or activated via different signaling pathways.

Citation: Jiang Z, Zhu S, Ye R, Xue Y, Chen A, et al. (2013) Relationship between NaCl- and H₂O₂-Induced Cytosolic Ca²⁺ Increases in Response to Stress in *Arabidopsis*. PLoS ONE 8(10): e76130. doi:10.1371/journal.pone.0076130

Editor: Gloria Muday, Wake Forest University, United States of America

Received: January 15, 2013; **Accepted:** August 27, 2013; **Published:** October 4, 2013

Copyright: © 2013 Jiang et al. This is an open-access article distributed under the terms of the Creative Commons Attribution License, which permits unrestricted use, distribution, and reproduction in any medium, provided the original author and source are credited.

Funding: ZJ and SZ were supported by fellowships from China Scholarship Council, Pandeng Project funds (PD11001008001; PD11002002004002) from Hangzhou Normal University, and a grant from Zhejiang NSF (Z3110443). This work is supported by grants from USDA (CSREES-2006-35100-17304) and from NSF (IOS-0848263) to ZMP. The funders had no role in study design, data collection and analysis, decision to publish, or preparation of the manuscript.

Competing interests: The authors have declared that no competing interests exist.

* E-mail: zpei@duke.edu

☯ These authors contributed equally to this work.

Introduction

The presence of high salinity affects almost every aspect of plant growth and development, and causes enormous losses in agricultural production worldwide. It is estimated that about 10 million hectares of agricultural land is abandoned every year because of high salinity, and salt stress affects as much as a quarter to a third of global agricultural land, particularly land which has been irrigated [1-3]. Given the continued increase in human population occurring in the world, it is estimated that crop production must be increased 50% by 2025 to stave off large-scale food shortages [4]. Thus, it is crucial to understand how plants respond to salt stress.

Many studies have been carried out to dissect the molecular and genetic mechanisms of the plant response to salt (NaCl)

stress, often using the model organism *Arabidopsis thaliana* [5-7]. Excess NaCl is toxic to plants, causing cellular ion imbalances and hyperosmotic stress [1-3,7]. NaCl stress also triggers a calcium signaling cascade in plants, leading to transcriptional regulation and subsequent physiological and developmental responses [1]. Although the molecular nature of initial perception of salt stress is unknown, it has been well established that salt stress triggers a transient increase in cytosolic Ca²⁺ concentration ([Ca²⁺]_i) that lasts about 2 min [8,9]. This increase has been proposed to represent a salt sensory process in plants [3,10].

In plants, Ca²⁺ as a secondary messenger is a key element to understanding a sophisticated network of signaling pathways responding to a large array of abiotic and biotic stimuli, including salt stress [11-13]. These specific Ca²⁺ signatures are

formed by the tightly regulated activities of Ca²⁺ channels and transporters in different tissues, organelles and membranes [13-16], and the changes in [Ca²⁺]_i are detected by cytosolic Ca²⁺ sensors. More than 250 Ca²⁺-binding EF-hand proteins have been identified in *Arabidopsis* [17], including the calmodulin (CaM), the calmodulin-like (CML), the Ca²⁺-dependent protein kinase (CDPK), and the calcineurin B-like (CBL) protein families. These cytosolic Ca²⁺ sensors decode and relay the information encoded within [Ca²⁺]_i signatures, allowing the plant to tightly bring about the appropriate adaptation to its ever-changing environment.

The salinity stress-induced increase in [Ca²⁺]_i leads to the activation of SOS3/CBL4, which functions as the primary Ca²⁺ sensor of [Ca²⁺]_i changes under salt stress [3]. Upon activation, SOS3/CBL4 interacts with the C-terminal region of a CBL-interacting protein kinase (CIPK) called SOS2/CIPK24, which in turn activates a plasma membrane Na⁺/H⁺ antiporter SOS1 that transports sodium ions out of the cell [3]. This salt signaling pathway reinforces the concept that the salt-induced [Ca²⁺]_i increase is an essential component for bringing about the plant response to salt stress.

Interestingly, after salt stress treatment there is an overproduction of reactive oxygen species (ROS), such as hydrogen peroxide (H₂O₂) [18-22]. The time constants for salt-induced increases in [Ca²⁺]_i and ROS are about 3 sec and 400 sec, respectively, as estimated from previous studies [8,21]. It appears that the increase in [Ca²⁺]_i occurs earlier than the ROS elevation after salt stress treatment. Considering ROS have also been shown to trigger increases in [Ca²⁺]_i [21,23-26], it is possible that ROS-induced [Ca²⁺]_i increases might serve as a feed forward mechanism in the salt stress signal transduction pathway. However, less is known about the relationship and interaction between the salt stress-induced [Ca²⁺]_i increases and the [Ca²⁺]_i increases evoked by ROS, which are produced in response to either salt stress specifically or other stresses in general [1,27].

In this study, we have systematically analyzed the relationship and interaction between salt stress-induced [Ca²⁺]_i increases and the ROS-induced [Ca²⁺]_i increases in *Arabidopsis*. We found the increases in [Ca²⁺]_i induced by both stimuli were higher than those induced by either single stress, suggesting that NaCl and H₂O₂ have an additive effect on [Ca²⁺]_i. We have also found that NaCl-induced [Ca²⁺]_i increases might inhibit both NaCl- and H₂O₂-gated channels by a feedback mechanism, but more NaCl-gated channels; a similar response was seen when the H₂O₂-induced [Ca²⁺]_i increases were analyzed. These data suggest responses seen involve both feedback inhibitory mechanisms, as well as an interaction between two stimuli-mediated Ca²⁺ signaling pathways.

Results

Dose-dependence and kinetics of NaCl- and H₂O₂-induced [Ca²⁺]_i increases

To analyze whether and how increases in [Ca²⁺]_i induced by NaCl and H₂O₂ interact each other in *Arabidopsis*, we attempted initially to identify optimum concentrations of NaCl and H₂O₂, which ideally could be applied to generate about half

of the maximum amplitude of [Ca²⁺]_i for potential up- and down-regulation. In addition, we attempted to establish the kinetics of NaCl- and H₂O₂-induced increases in [Ca²⁺]_i for administering these stresses in different sequential combinations. First, to analyze NaCl-induced increases in [Ca²⁺]_i, we treated *Arabidopsis* seedlings expressing aequorin with solutions containing 0 to 600 mM NaCl. Aequorin bioluminescence images were taken every 10 sec for 500 sec, and the peak [Ca²⁺]_i was calculated and analyzed, as NaCl induces a transient increase in [Ca²⁺]_i [8,9]. Plants grown on the half-strength MS medium had an average basal [Ca²⁺]_i of 80 ± 21 nM (Figure 1A and C). As expected, the [Ca²⁺]_i increased in response to NaCl treatment (Figure 1A). The magnitudes of [Ca²⁺]_i increases were dependent on the concentration of NaCl, higher concentration of NaCl evoked a larger increase in [Ca²⁺]_i. The NaCl concentration needed for a half-maximal response was ~200 mM, which was chosen as an optimum concentration to subsequently analyze the interaction with H₂O₂-induced increases in [Ca²⁺]_i.

Then, we determined the temporal dynamics of NaCl-induced [Ca²⁺]_i increases under the imposed experimental conditions as a control for further comparison (Figure 1B). We found that [Ca²⁺]_i increased immediately after the application of 200 mM NaCl, reached a peak of ~1 μM at about 20 sec, and then declined gradually (Figure 1B). Note that, the peaking time might be shorter than 20 sec based on previous studies [8,9]. Nevertheless, imaging aequorin bioluminescence for less than 10 sec resulted in images with low a signal-noise ratio in our system. Thus, the temporal resolution was about 10 sec, which is sufficient for the current study. At about 200 sec, the [Ca²⁺]_i was reduced to a new resting level of under 200 nM.

Similarly, we analyzed increases in [Ca²⁺]_i in response to H₂O₂. Seedlings were treated with different concentrations of H₂O₂ from 0 to 15 mM and [Ca²⁺]_i was analyzed. As expected, H₂O₂ induced increases in [Ca²⁺]_i in a dose-dependent manner (Figure 1C). The H₂O₂ concentration for a half-maximal response was around 4 mM with the magnitude of [Ca²⁺]_i similar to that induced by 200 mM NaCl. We then determined the temporal dynamics of the [Ca²⁺]_i increase induced by 4 mM H₂O₂. Following treatment with 4 mM H₂O₂, [Ca²⁺]_i increased and reached a peak of ~1 μM at 50 sec (Figure 1D). It took another 100 sec for the [Ca²⁺]_i to reach a new basal level of just under 200 nM. Taken together, it seems that increases in [Ca²⁺]_i occur faster in response to NaCl than H₂O₂, but are reset to a resting level 150 sec after treatment.

Additive effect of NaCl and H₂O₂ on triggering increases in [Ca²⁺]_i

To investigate thoroughly the relationship and/or interaction between [Ca²⁺]_i increases triggered by NaCl and H₂O₂, *Arabidopsis* seedlings were treated with 200 mM NaCl or 4 mM H₂O₂ separately, or 200 mM NaCl together with 4 mM H₂O₂. Note that, although salt-induced ROS production could be detected within ~2 min after salt treatment [21] the estimated half-time to the peak of ROS production is more than 5 min. Note also that, we did not detect a second peak of [Ca²⁺]_i within 5 min after salt stress treatment (Figure S1A), suggesting that salt-induced ROS could not trigger a detectable increase in

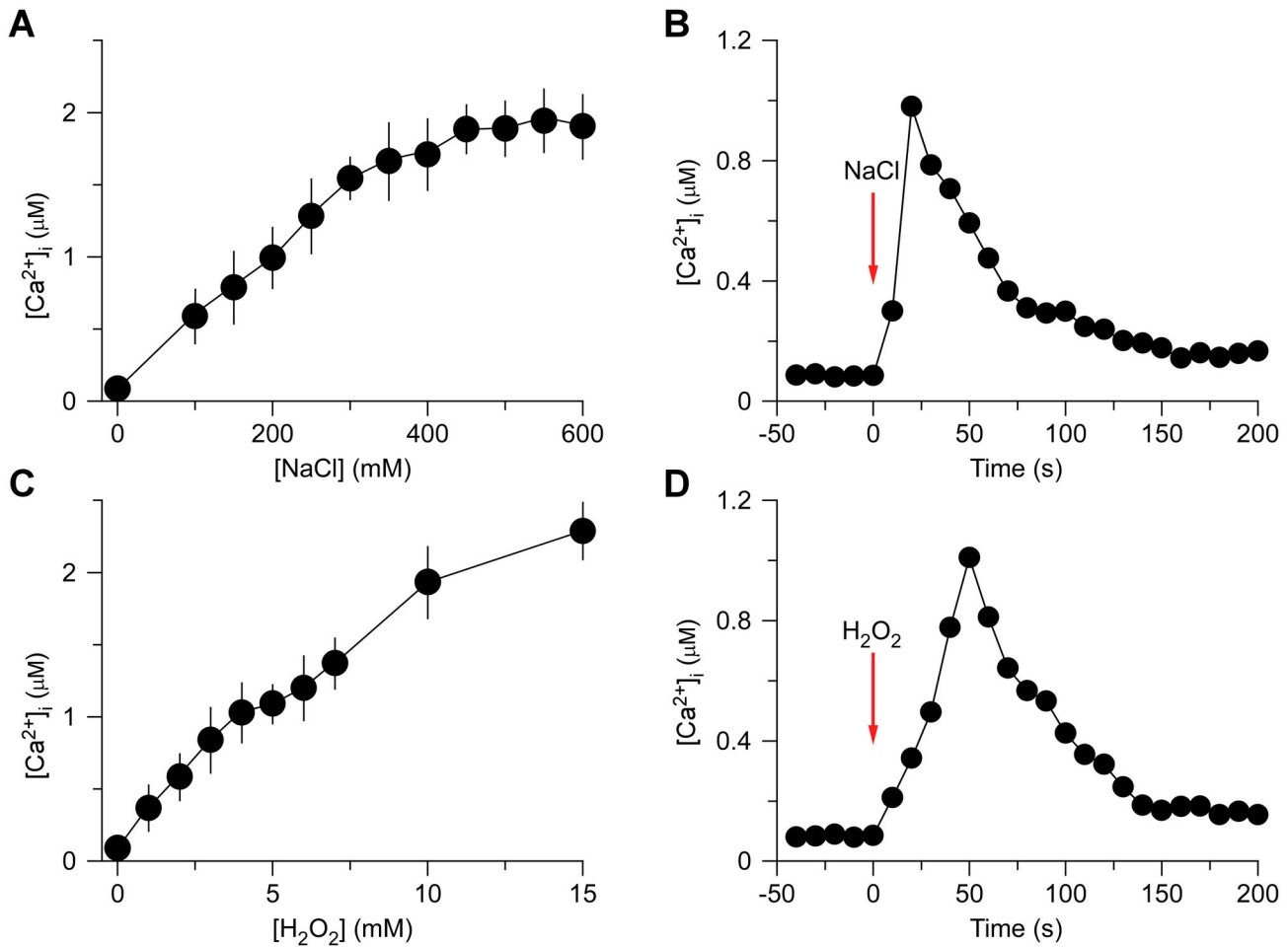


Figure 1. Increases in [Ca²⁺]_i in response to NaCl and H₂O₂ treatments. (A and C) Increases in [Ca²⁺]_i induced by several concentrations of NaCl (A) and H₂O₂ (C) in *Arabidopsis*. Seedlings expressing aequorin and grown for 7 days were treated with solutions containing several concentrations of NaCl or H₂O₂, and aequorin images were taken every 10 sec for 500 sec. Data for four independent experiments are shown (mean ± sem; *n* = 64). (B and D) Time courses of increases in [Ca²⁺]_i induced by 200 mM NaCl (B) or 4 mM H₂O₂ (D). Seedlings grown for 7 days were treated with NaCl and H₂O₂ at time zero, and aequorin images were taken every 10 sec. Representative recordings from individual seedlings were shown. Similar results were seen in six independent experiments using 128 seedlings.

doi: 10.1371/journal.pone.0076130.g001

[Ca²⁺]_i under the current experimental conditions. Because we measured [Ca²⁺]_i changes within 5 min after salt treatment, the effect of salt-induced ROS on [Ca²⁺]_i should not interfere apparently. The [Ca²⁺]_i increases recorded after single treatments were consistent with the results described above (Figure 2A–C). NaCl and H₂O₂ induced similar increases in [Ca²⁺]_i (Figure 2E). When plants were treated with both stimuli simultaneously, the peaks of [Ca²⁺]_i were much larger than that induced by each individual stimulus (Figure 2D and E), showing an additive effect. To further analyze how salt-induced ROS affects [Ca²⁺]_i increases in response to salt stress within 500 sec, we carried out an experiment by using the NADPH oxidase inhibitor DPI [28] and ROS scavengers ascorbic acid and glutathione [27], and found that neither of these reagents significantly affected [Ca²⁺]_i increases induced by NaCl (Figure

S1). These results suggest that the NaCl- and H₂O₂-induced [Ca²⁺]_i increases may be largely independent events. In other words, NaCl and H₂O₂ might activate different Ca²⁺ permeable channels.

The crosstalk between NaCl- and H₂O₂-induced [Ca²⁺]_i increases

To further characterize the potential interaction between the two stimuli-triggered [Ca²⁺]_i signals, plants were successively treated either with the same stimulus or the other. When the *Arabidopsis* seedlings were treated with 200 mM NaCl, the level of [Ca²⁺]_i increased quickly to reach a peak and decreased to the new resting level after 150 sec (Figure 3A), as described in Figure 1B. A subtle increase in [Ca²⁺]_i could be detected in seedlings after washing with deionized water at 200

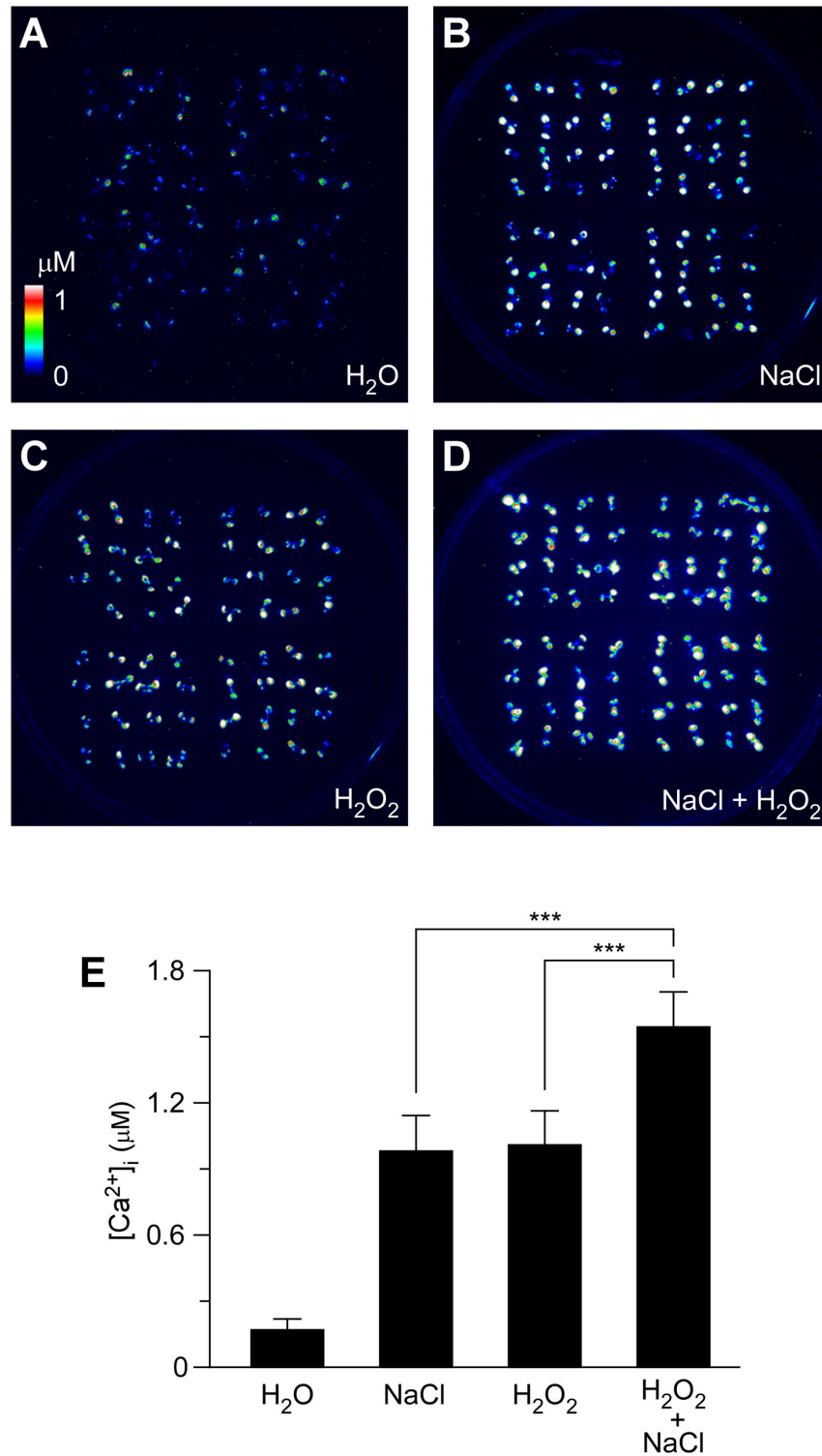


Figure 2. Increases in [Ca²⁺]_i in response to NaCl and H₂O₂ individually or combined. (A to D) Imaging of [Ca²⁺]_i increases in response to the treatments of water (H₂O; A), 200 mM NaCl (B), 4 mM H₂O₂ (A), and 200 mM NaCl and 4 mM H₂O₂ together (D) in *Arabidopsis* seedlings expressing aequorin. [Ca²⁺]_i increases were analyzed by imaging bioluminescence and scaled by a pseudo-color bar.

(E) Quantification of [Ca²⁺]_i increases from experiments as in (A) to (D). Data for four independent experiments are shown (mean ± sd; $n = 64$; *** $P < 0.001$; NS, not significant $P > 0.05$).

doi: 10.1371/journal.pone.0076130.g002

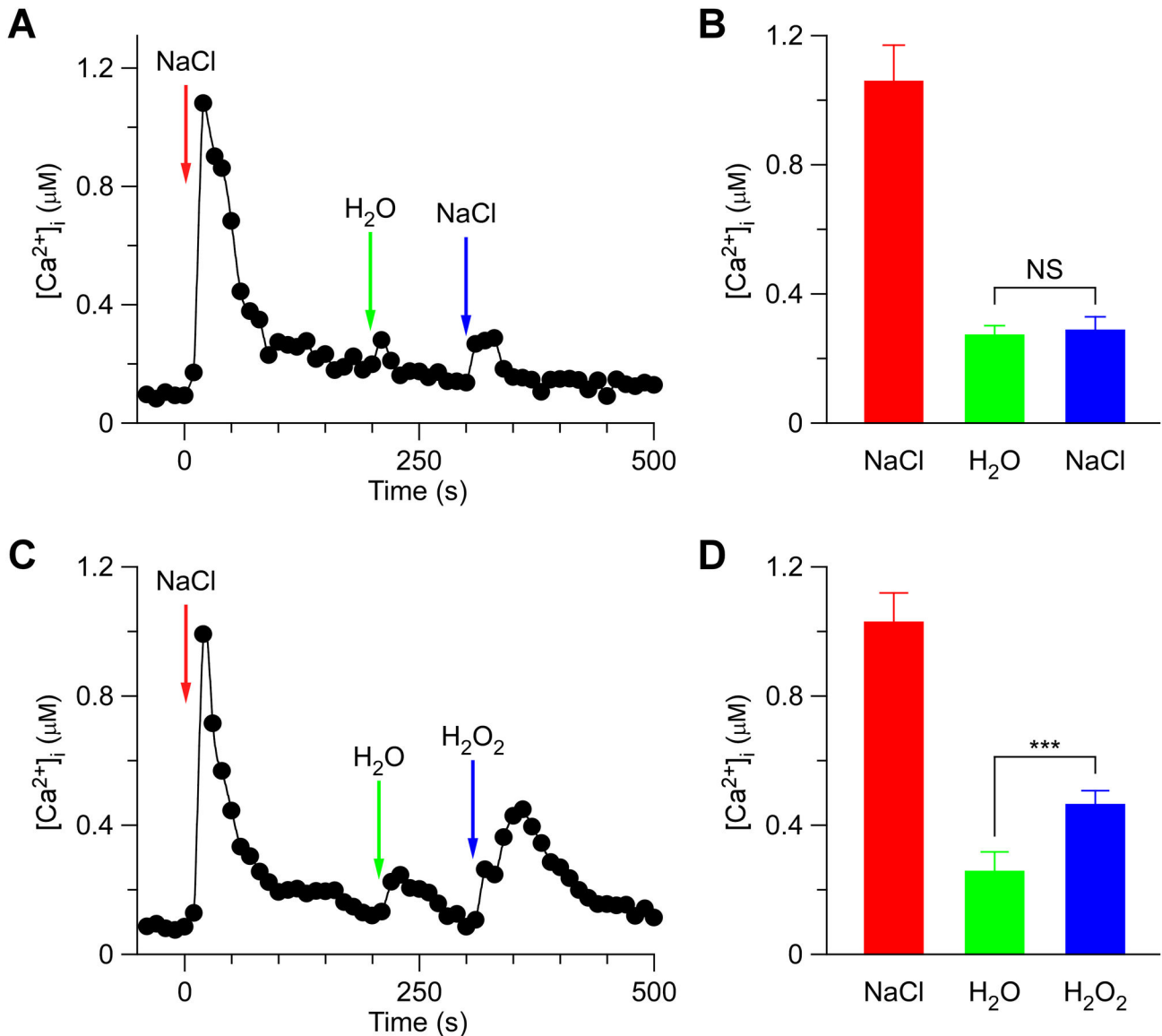


Figure 3. NaCl-induced $[Ca^{2+}]_i$ increases inhibits NaCl-activated channels more than H₂O₂-activated channels. (A and C) *Arabidopsis* seedlings were subjected to a 200 mM NaCl treatment once at 0 sec, and the solution was perfused by deionized water at 200 sec. Then, a second 200 mM NaCl (A), or 4 mM H₂O₂ (C) treatment was applied around 300 sec. Aequorin luminescence was recorded continuously through the treatments in the dark.

(B and D) Quantification of $[Ca^{2+}]_i$ increases for the 2nd NaCl (B) or 2nd H₂O₂ treatment (C) from experiments as in (A) to (C), respectively. Data for four independent experiments are shown (mean \pm sd; $n = 64$; NS, not significant $P > 0.05$; *** $P < 0.001$).

doi: 10.1371/journal.pone.0076130.g003

sec (Figure 3A and B; green). Then, NaCl was added again, which caused a small increase in $[Ca^{2+}]_i$. It decayed from 300 sec to a level similar to the previous resting level (Figure 3A and B). Compared to the first NaCl treatment, which led to a large $[Ca^{2+}]_i$ increase to $\sim 1 \mu\text{M}$, the 2nd NaCl treatment resulted in a $[Ca^{2+}]_i$ increase that was only a fraction of the size of the first $[Ca^{2+}]_i$ increase. This observation suggests that the NaCl-activated Ca²⁺ permeable channel (NaC) might be desensitized or adapted by unknown signaling elements upstream of NaC

activation. To test whether the NaC is desensitized or adapted, we waited for 3 hr and were able to detect a normal ($\sim 1 \mu\text{M}$) $[Ca^{2+}]_i$ increase in response to NaCl, suggesting that the NaC is most likely desensitized (data not shown).

Subsequently we analyzed whether the hydrogen peroxide-activated Ca²⁺ permeable channel (HpC) was affected by the initial NaCl treatment. The second NaCl treatment was replaced by 4 mM H₂O₂ at 300 sec (Figure 3C). Interestingly, the peak of $[Ca^{2+}]_i$ induced by H₂O₂ was clearly greater than

that induced by 200 mM NaCl ($P < 0.001$). After 450 sec, the [Ca²⁺]_i decreased to a new basal level under 200 μM (Figure 3C and D). The lower inhibition of HpC than NaC by the initial NaCl treatment suggests that the initial high level of [Ca²⁺]_i, which resulted from NaC activation (called ^{NaC}[Ca²⁺]_i microdomain/puff) subsequently inhibited NaC more than HpC (Figure 3).

By analogy, we used H₂O₂ as the first stimuli to treat the seedlings and then analyzed the second treatment using H₂O₂ or NaCl (Figure 4). When H₂O₂ was added to the Petri dish, at 300 sec after the first H₂O₂ treatment, the [Ca²⁺]_i level stabilized at 178 ± 32 nM, similar to previous resting levels (Figure 4A and B). But when we used 200 mM NaCl to replace H₂O₂ at 300 sec, the peak values of [Ca²⁺]_i were 381 ± 23 nM, small but significantly higher than that seen with the second H₂O₂ treatment (Figure 4B and D). Similarly, our results suggest that the high [Ca²⁺]_i, which resulted from the initial HpC activation (called ^{HpC}[Ca²⁺]_i microdomain), inhibited HpC more than NaC (Figures 4 and 5).

Discussion

Calcium is a universal second messenger that plays an important role in signal transduction in animals and plants [25,29-31]. In the past 20 years, tremendous progress has been made in understanding the changes in [Ca²⁺]_i that appear in response to various abiotic and biotic stresses in plants, including salt stress, oxidative stress, drought, high and low temperatures, and pathogen elicitors [13,25,26,32]. It is known that a specific stimulus can trigger unique temporal and spatial patterns of [Ca²⁺]_i, also known as [Ca²⁺]_i signatures [33]. The [Ca²⁺]_i signature encodes information from the environmental stimulus which will be decoded subsequently by intracellular Ca²⁺ sensors, such as calmodulins (CaMs) and calcineurin B-like proteins (CBLs), leading to the activation of downstream events [10]. It is also known that the basal [Ca²⁺]_i is maintained at a concentration about 10,000-fold below the extracellular Ca²⁺ concentration [29,31,34]. In general, Ca²⁺ channels in the plasma membrane and/or endomembranes are activated in response to environmental stimuli, leading to increases in [Ca²⁺]_i [30,32]. Salt stress-induced increases in [Ca²⁺]_i have long been proposed as being involved in the process perceiving the salt signal although the properties of the salt-activated Ca²⁺ permeable channel are poorly understood and its molecular nature remains to be identified [1,2,7].

In addition, various abiotic and biotic stresses lead to the production of ROS and oxidative stresses, which control many different processes in plants [27,35-37]. It has been well established that salt stress enhances the production of reactive oxygen species (ROS) in plants [18-22]. Interestingly, ROS has also been shown to activate Ca²⁺ permeable channels in the plasma membrane, which in turn lead to Ca²⁺ influx into the cell and thus increases in [Ca²⁺]_i [19,24,38]. Note that, the salt stress-induced [Ca²⁺]_i increases precede the production of H₂O₂ signaling molecule [39]. Nevertheless, little is known about the molecular mechanisms underlying ROS perception in plant cells, and it is possible that ROS activation of Ca²⁺ permeable channels may serve as a ROS perception process.

The decay of the increases in [Ca²⁺]_i induced by both NaCl and H₂O₂ seen in this study (Figure 1B and D) as well as previous studies [8,9,15] indicates that the stimulus-activated Ca²⁺ permeable channels may be inactivated via a feedback inhibitory mechanism, i.e. elevated [Ca²⁺]_i inhibits these channels, a desensitization process commonly seen for receptor ion channels in animals [31,40]. It remains to be addressed whether the localized increases in [Ca²⁺]_i induced by one stimulus, called [Ca²⁺]_i microdomain [29,31], inhibit the other stimulus-activated Ca²⁺ permeable channels. It is known that NaCl induces multiple peaks of [Ca²⁺]_i under certain conditions [9], possibly because the same NaCl-sensitive channels are repetitively activated, or that NaCl might trigger H₂O₂ production which subsequently activates another Ca²⁺ channel, different from the NaCl-sensitive channel. Under our experimental conditions, we did not observe multiple peaks of [Ca²⁺]_i after salt treatment (Figure S1A).

NaCl and H₂O₂ together induced larger increases in [Ca²⁺]_i than either NaCl or H₂O₂ alone (Figure 2), suggesting that NaCl and H₂O₂ may activate distinct Ca²⁺ permeable channels, NaC and HpC (Figure 5). NaC and HpC are likely regulated by feedback inhibition (Figure 5), considering their desensitization seen in this study (Figure 1B and D) as well as previous reports [8,9]. We demonstrated that repetitive NaCl treatments failed to trigger repetitive [Ca²⁺]_i increases (Figure 3A and B). This indicates that the NaC cannot be activated repetitively within a short period of time, i.e. NaC is possibly desensitized. We propose that a feedback inhibition may be involved in the desensitization (Figure 5). Upon NaCl treatment, the NaC opens, leading to the localized increase of [Ca²⁺]_i, ^{NaC}[Ca²⁺]_i microdomain/puff. ^{NaC}[Ca²⁺]_i in turn signals the channel to close, which prevents further [Ca²⁺]_i increases and allows the basal [Ca²⁺]_i to be reset via Ca²⁺ pumps. This feedback inhibition avoids the excessive increase of [Ca²⁺]_i which could be disastrous to plant cells. The same phenomenon was also observed with the activation of HpC (Figure 5), i.e. ^{HpC}[Ca²⁺]_i microdomain inhibits HpC via a feedback mechanism. Clearly, the most significant effect is that after the initial treatment by either NaCl or H₂O₂, [Ca²⁺]_i increases induced by both NaCl and H₂O₂ are reduced (Figures 3 and 4). It is most likely that localized ^{NaC}[Ca²⁺]_i and ^{HpC}[Ca²⁺]_i merge to form a relatively global [Ca²⁺]_i, which then feedback inhibits both NaC and HpC (Figure 5). We observed that *Arabidopsis* was unable to recover from 200 mM NaCl treatment 5 min after an initial stimulation. Similar results were observed after 4 mM H₂O₂ treatment. In contrast, a previous study has shown that *Arabidopsis* is able to recover its ability to respond almost fully to cold shock 3 min after an initial cold shock [41]. Note that, our work does not prove that HpC and NaC are localized in discreet and different microdomains in the plasma membrane, rather we have shown HpC and NaC may differ and interact via [Ca²⁺]_i microdomains. It is also possible that NaCl and H₂O₂ may activate the same Ca²⁺ permeable channel, which is expressed in different types of cells and/or activated via different signaling pathways, leading to the differential changes in [Ca²⁺]_i.

In general, when plants are exposed to one stress, their resistance to other stresses can be enhanced. It is most likely

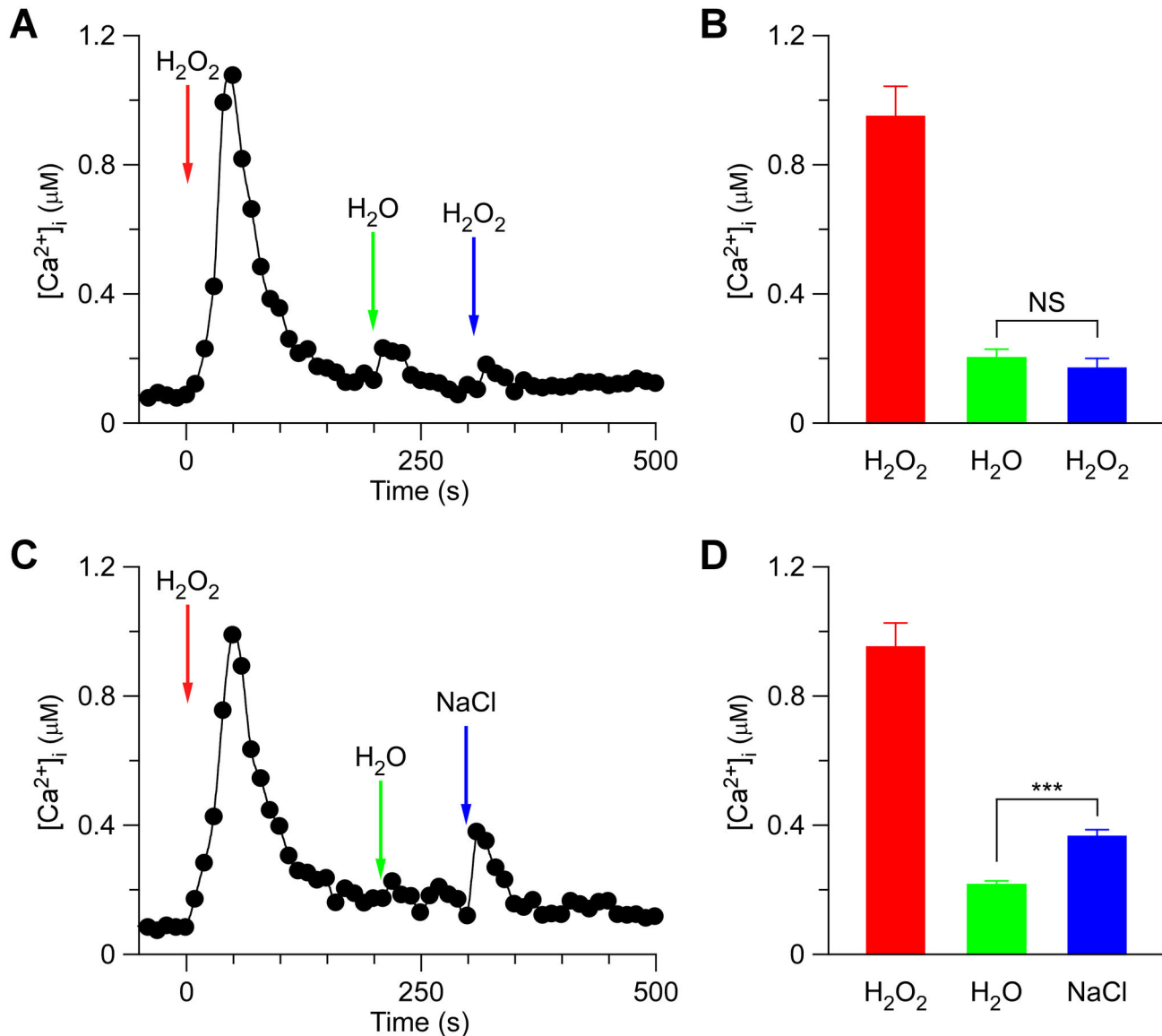


Figure 4. H₂O₂-induced [Ca²⁺]_i increases inhibits H₂O₂-activated channels more than NaCl-activated channels. (A and C) *Arabidopsis* seedlings were subjected to a 4 mM H₂O₂ treatment once at 0 sec, and the solution was perfused by deionized water at 200 sec. Then, a second 4 mM H₂O₂ (A), or 200 mM NaCl (C) treatment was applied around 300 sec. Aequorin luminescence was recorded continuously through the treatments in the dark.

(B and D) Quantification of [Ca²⁺]_i increases for the 2nd H₂O₂ (B) or 2nd NaCl treatment (C) from experiments as in (A) to (C), respectively. Data for four independent experiments are shown (mean ± sd; n = 64; NS, not significant P > 0.05; *** P < 0.001).

doi: 10.1371/journal.pone.0076130.g004

that stress-evoked [Ca²⁺]_i increases as well as stress-stimulated overproduction of ROS function as key integrators, possibly mediating stress signal perception and signal transduction. Our results demonstrate the inhibitory interaction of NaCl- and H₂O₂-induced [Ca²⁺]_i increases, and may predict distinct Ca²⁺ permeable channels activated by NaCl and H₂O₂, respectively (Figure 5). In the future, it is important to analyze the pharmacological properties of these putative Ca²⁺ permeable channels activated by NaCl and H₂O₂ as described

previously for MAMP-activated channels [42]. Obviously, the identification of these channels or sensors will be a hallmark in the study of plant salt resistance in the future. In addition, how NaC and HpC interact to contribute to the [Ca²⁺]_i signatures and other downstream events can be further analyzed when their molecular nature is identified.

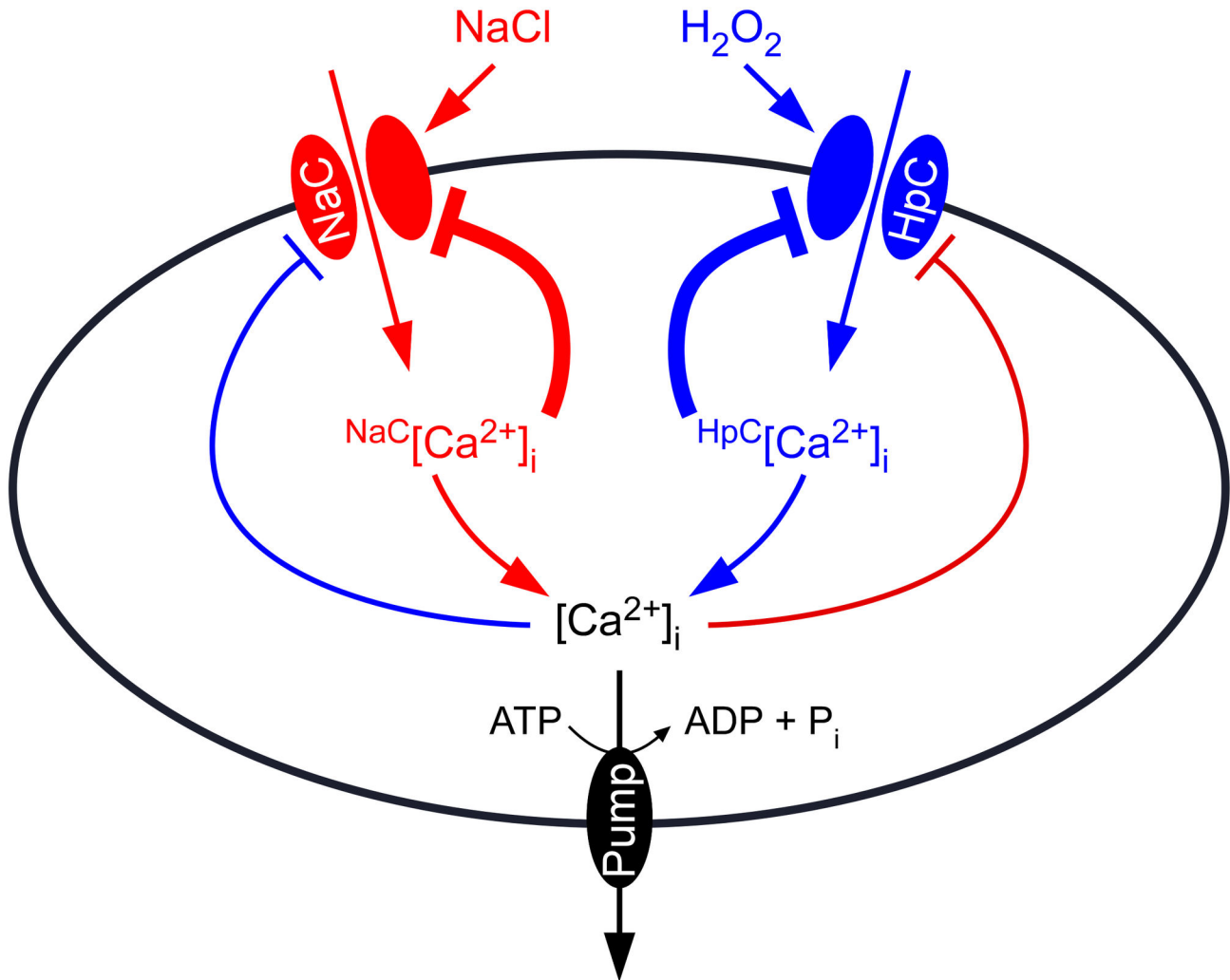


Figure 5. Model for the interaction between NaCl- and H₂O₂-induced [Ca²⁺]_i increases. A Ca²⁺ channel activated by NaCl (NaC) results in localized [Ca²⁺]_i increases, called NaC-related [Ca²⁺]_i microdomain (^{NaC}[Ca²⁺]_i). ^{NaC}[Ca²⁺]_i feedback inhibits the activity of NaC. HpC, a Ca²⁺ channel activated by hydrogen peroxide, leads to localized [Ca²⁺]_i increases, called ^{HpC}[Ca²⁺]_i microdomain. ^{HpC}[Ca²⁺]_i also feedback inhibits HpC activity. The [Ca²⁺]_i microdomain-mediated inhibition of Ca²⁺ channels is the major feedback inhibitory pathways (thick lines). In addition, both ^{NaC}[Ca²⁺]_i and ^{HpC}[Ca²⁺]_i might contribute to a global [Ca²⁺]_i increase, which further inhibits both NaC and HpC, serving as global feedback inhibitory pathways (thin lines). [Ca²⁺]_i is reset to the resting level by plasma membrane Ca²⁺ pumps.

doi: 10.1371/journal.pone.0076130.g005

Materials and Methods

Plant materials and growth conditions

Arabidopsis thaliana ecotype Columbia-0 (Col-0) constitutively expressing intracellular aequorin (pMAQ2, a kind gift from Dr. M. Knight) under the control of the cauliflower mosaic virus 35S promoter was used [8,33]. *Arabidopsis* plants were grown in 150 mm x 15 mm round Petri dishes in half-strength Murashige and Skoog salts (MS; Gibco), supplemented with 1.5% (w/v) sucrose (Sigma), and 0.8% (w/v) agar (Becton Dickinson) adjusted to pH 6.0 with KOH in controlled environmental rooms at 21 ± 2°C. The fluency rate of

white light was ~110 μmol m⁻² sec⁻¹. The photoperiods were 16 h light/8 h dark cycles. Seeds were sterilized with 2.5% PPM (Plant preservative mixture; Caisson Laboratories) and stratified at 4°C for 3 days in the dark, and then transferred to growth rooms.

Aequorin reconstitution and measurement of [Ca²⁺]_i

Arabidopsis thaliana plants expressing cytosolic apoaequorin were used for [Ca²⁺]_i measurements [33,43]. Seedlings were grown on half-strength Murashige and Skoog medium for 7 days. Reconstitution of aequorin was performed *in vivo* by spraying seedlings with 240 μL of 10 μM coelenterazine per

Petri dish followed by incubation at 21°C in the dark for 8 hr. Treatments and aequorin luminescence imaging were performed at room temperature using a ChemiPro HT system that includes a cryogenically cooled and back-illuminated CCD camera, liquid nitrogen autofiller, camera controller, and computer-equipped WinView/32 software (Roper Scientific) as described previously [33]. The CCD camera has a 1300 × 1340 pixel resolution and is cooled to -110°C by the cryogenic cooler system prior to image recording. The recording was started 50 s prior treatments and luminescence images were taken every 10 sec. The total remaining aequorin was estimated by treating plants with a discharging solution containing 0.9 M CaCl₂ in 10% (v/v) ethanol and recorded for 5 min until values were within 1% of the highest discharge value [8,15,33]. WinView/32 and Meta Morph 6 were used to analyze recorded luminescence images. Experiments were carried out at room temperature (22 to 24°C).

NaCl and H₂O₂ treatments

For stress treatments, Petri dishes were placed individually into the ChemiPro HT chamber and luminescence images were taken at 10 sec intervals starting 50 sec prior the treatment. The treatment solution (100 mL) at described concentrations of NaCl or H₂O₂ was added into Petri dish in the dark, and luminescence was recorded continuously. For changes in bath solution, a four-channel peristaltic pump (Dynamax RP-1, Rainin) was used to perfuse Petri dish with water as indicated in the figures. Then, additional stress treatment was applied by adding 100 mL solution into Petri dish.

Calibration of calcium measurements

The cytosolic free cytosolic Ca²⁺ concentrations were calculated based on the calibration equation described previously [41] with modification to the ChemiPro system. The wild-type *Arabidopsis* expressing aequorin were placed individually in each well in 96-well plates containing ½ MS medium, 1.5% (w/v) sucrose, and 0.8% (w/v) agar for 10 days. Kinetic luminescence measurements were performed with an automated microplate luminescence reader (*Mithras* LB 940, Berthold Technologies). After automatic injection of 0.2 ml of solution into the each well bioluminescence counts were integrated every 1 sec as described previously [41]. The

solutions containing a range of [NaCl] from 0 to 600 mM were used to treat the plants, and the peak values of [Ca²⁺]_i were calculated used the equation described previously [41]. Similar measurements were carried out using the ChemiPro HT system as described above to obtain L/L_{max} values for each treatment, where L is luminescence and L_{max} is the total remaining counts for bioluminescence. Then, we fit these data to the previously describe equation $pCa = a * (-\log(L/L_{max})) + b$, and obtained the equation $pCa = 0.9057209 * (-\log(L/L_{max})) + 4.7712743$. Note that, the calculated Ca²⁺ concentrations presented in the current study are similar to those reported previously [8,41].

Supporting Information

Figure S1. H₂O₂ levels do not affect [Ca²⁺]_i increases in response to NaCl treatment. (A) *Arabidopsis* seedlings were treated with water (Control), the NADPH oxidase inhibitor DPI (15 μM), and ROS scavenger ascorbic acid (5 mM) and glutathione (5 mM) two hours prior to the NaCl treatment. The seedlings were then subjected to a 200 mM NaCl treatment, and aequorin luminescence was recorded continuously through the treatments in the dark. (B) Quantification of peak [Ca²⁺]_i increases from experiments as in (A). Data for three independent experiments are shown (mean ± sd; n = 35 to 62; NS, not significant, P > 0.05). (PDF)

Acknowledgements

We thank Marc R. Knight for *Arabidopsis* seeds expressing aequorin, James N. Siedow for discussion and critical reading of the manuscript, Douglas M. Johnson and Gary B. Swift for maintenance of the ChemiPro system, and the Pei lab members for discussion and support.

Author Contributions

Conceived and designed the experiments: ZMP ZJ. Performed the experiments: ZJ SZ RY YX AC. Analyzed the data: ZJ RY ZMP. Contributed reagents/materials/analysis tools: RY YX LA. Wrote the manuscript: ZMP ZJ.

References

- Munns R, Tester M (2008) Mechanisms of salinity tolerance. *Annu Rev Plant Biol* 59: 651-681. doi:10.1146/annurev.arplant.59.032607.092911. PubMed: 18444910.
- Zhu JK (2001) Plant salt tolerance. *Trends Plant Sci* 6: 66-71. doi: 10.5363/tits.6.11_66. PubMed: 11173290.
- Zhu JK (2003) Regulation of ion homeostasis under salt stress. *Curr Opin Plant Biol* 6: 441-445. doi:10.1016/S1369-5266(03)00085-2. PubMed: 12972044.
- Flowers TJ (2004) Improving crop salt tolerance. *J Exp Bot* 55: 307-319. doi:10.1093/jxb/erh003. PubMed: 14718494.
- Qiu QS, Guo Y, Dietrich MA, Schumaker KS, Zhu JK (2002) Regulation of SOS1, a plasma membrane Na⁺/H⁺ exchanger in *Arabidopsis thaliana*, by SOS2 and SOS3. *Proc Natl Acad Sci U S A* 99: 8436-8441. doi:10.1073/pnas.122224699. PubMed: 12034882.
- Shi H, Ishitani M, Kim C, Zhu JK (2000) The *Arabidopsis thaliana* salt tolerance gene SOS1 encodes a putative Na⁺/H⁺ antiporter. *Proc Natl Acad Sci U S A* 97: 6896-6901. doi:10.1073/pnas.120170197. PubMed: 10823923.
- Luan S, Lan W, Chul Lee S (2009) Potassium nutrition, sodium toxicity, and calcium signaling: connections through the CBL-CIPK network. *Curr Opin Plant Biol* 12: 339-346. doi:10.1016/j.pbi.2009.05.003. PubMed: 19501014.
- Knight H, Trewavas AJ, Knight MR (1997) Calcium signalling in *Arabidopsis thaliana* responding to drought and salinity. *Plant J* 12: 1067-1078. doi:10.1046/j.1365-313X.1997.12051067.x. PubMed: 9418048.
- Tracy FE, Gilliam M, Dodd AN, Webb AA, Tester M (2008) NaCl-induced changes in cytosolic free Ca²⁺ in *Arabidopsis thaliana* are heterogeneous and modified by external ionic composition. *Plant Cell Environ* 31: 1063-1073. doi:10.1111/j.1365-3040.2008.01817.x. PubMed: 18419736.

10. Luan S (2009) The CBL-CIPK network in plant calcium signaling. *Trends Plant Sci* 14: 37-42. doi:10.1016/j.tplants.2008.10.005. PubMed: 19054707.
11. Hetherington AM, Brownlee C (2004) The generation of Ca(2+) signals in plants. *Annu Rev Plant Biol* 55: 401-427. doi:10.1146/annurev.arplant.55.031903.141624. PubMed: 15377226.
12. Pandey GK, Cheong YH, Kim KN, Grant JJ, Li L et al. (2004) The calcium sensor calcineurin B-like 9 modulates abscisic acid sensitivity and biosynthesis in *Arabidopsis*. *Plant Cell* 16: 1912-1924. doi:10.1105/tpc.021311. PubMed: 15208400.
13. Dodd AN, Kudla J, Sanders D (2010) The language of calcium signaling. *Annu Rev Plant Biol* 61: 593-620. doi:10.1146/annurev-arplant-070109-104628. PubMed: 20192754.
14. Kudla J, Batistic O, Hashimoto K (2010) Calcium signals: the lead currency of plant information processing. *Plant Cell* 22: 541-563. doi:10.1105/tpc.109.072686. PubMed: 20354197.
15. Rentel MC, Knight MR (2004) Oxidative stress-induced calcium signaling in *Arabidopsis*. *Plant Physiol* 135: 1471-1479. doi:10.1104/pp.104.042663. PubMed: 15247375.
16. Batistić O, Kudla J (2012) Analysis of calcium signaling pathways in plants. *Biochim Biophys Acta* 1820: 1283-1293. doi:10.1016/j.bbagen.2011.10.012. PubMed: 22061997.
17. Day IS, Reddy VS, Shad Ali G, Reddy AS (2002) Analysis of EF-hand-containing proteins in *Arabidopsis*. *Genome Biol* 3: RESEARCH0056. PubMed: 12372144.
18. Borsani O, Zhu J, Verslues PE, Sunkar R, Zhu JK (2005) Endogenous siRNAs derived from a pair of natural cis-antisense transcripts regulate salt tolerance in *Arabidopsis*. *Cell* 123: 1279-1291. doi:10.1016/j.cell.2005.11.035. PubMed: 16377568.
19. Miller G, Suzuki N, Ciftci-Yilmaz S, Mittler R (2010) Reactive oxygen species homeostasis and signalling during drought and salinity stresses. *Plant Cell Environ* 33: 453-467. doi:10.1111/j.1365-3040.2009.02041.x. PubMed: 19712065.
20. Vaidyanathan H, Sivakumar P, Chakrabarty R, Thomas G (2003) Scavenging of reactive oxygen species in NaCl-stressed rice (*Oryza sativa* L.) - differential response in salt-tolerant and sensitive varieties. *Plant Sci* 165: 1411-1418. doi:10.1016/j.plantsci.2003.08.005.
21. Leshem Y, Seri L, Levine A (2007) Induction of phosphatidylinositol 3-kinase-mediated endocytosis by salt stress leads to intracellular production of reactive oxygen species and salt tolerance. *Plant J* 51: 185-197. doi:10.1111/j.1365-3113.2007.03134.x. PubMed: 17521408.
22. Valderrama R, Corpas FJ, Carreras A, Gómez-Rodríguez MV, Chaki M et al. (2006) The dehydrogenase-mediated recycling of NADPH is a key antioxidant system against salt-induced oxidative stress in olive plants. *Plant Cell Environ* 29: 1449-1459. doi:10.1111/j.1365-3040.2006.01530.x. PubMed: 17080966.
23. McAinsh MR, Clayton H, Mansfield TA, Hetherington AM (1996) Changes in stomatal behavior and guard cell cytosolic free calcium in response to oxidative stress. *Plant Physiol* 111: 1031-1042. PubMed: 12226345.
24. Pei ZM, Murata Y, Benning G, Thomine S, Klüsener B et al. (2000) Calcium channels activated by hydrogen peroxide mediate abscisic acid signalling in guard cells. *Nature* 406: 731-734. doi:10.1038/35021067. PubMed: 10963598.
25. McAinsh MR, Pittman JK (2009) Shaping the calcium signature. *New Phytol* 181: 275-294. doi:10.1111/j.1469-8137.2008.02682.x. PubMed: 19121028.
26. Ma W, Berkowitz GA (2011) Ca²⁺ conduction by plant cyclic nucleotide gated channels and associated signaling components in pathogen defense signal transduction cascades. *New Phytol* 190: 566-572. doi:10.1111/j.1469-8137.2010.03577.x. PubMed: 21166809.
27. Suzuki N, Koussevitzky S, Mittler R, Miller G (2012) ROS and redox signalling in the response of plants to abiotic stress. *Plant Cell Environ* 35: 259-270. doi:10.1111/j.1365-3040.2011.02336.x. PubMed: 21486305.
28. Marino D, Dunand C, Puppo A, Pauly N (2012) A burst of plant NADPH oxidases. *Trends Plant Sci* 17: 9-15. doi:10.1016/j.tplants.2011.10.001. PubMed: 22037416.
29. Clapham DE (2007) Calcium signaling. *Cell* 131: 1047-1058. doi:10.1016/j.cell.2007.11.028. PubMed: 18083096.
30. Ward JM, Mäser P, Schroeder JI (2009) Plant ion channels: gene families, physiology, and functional genomics analyses. *Annu Rev Physiol* 71: 59-82. doi:10.1146/annurev.physiol.010908.163204. PubMed: 18842100.
31. Berridge MJ, Bootman MD, Roderick HL (2003) Calcium signalling: dynamics, homeostasis and remodelling. *Nat Rev Mol Cell Biol* 4: 517-529. doi:10.1038/nrm1155. PubMed: 12838335.
32. Hetherington AM, Brownlee C (2004) The generation of Ca²⁺ signals in plants. *Annu Rev Plant Biol* 55: 401-427. doi:10.1146/annurev.arplant.55.031903.141624. PubMed: 15377226.
33. Tang RH, Han S, Zheng H, Cook CW, Choi CS et al. (2007) Coupling diurnal cytosolic Ca²⁺ oscillations to the CAS-IP₃ pathway in *Arabidopsis*. *Science* 315: 1423-1426. doi:10.1126/science.1134457. PubMed: 17347443.
34. Swanson SJ, Choi WG, Chanoca A, Gilroy S (2011) In vivo imaging of Ca²⁺, pH, and reactive oxygen species using fluorescent probes in plants. *Annu Rev Plant Biol* 62: 273-297. doi:10.1146/annurev-arplant-042110-103832. PubMed: 21370977.
35. Vranová E, Inzé D, Van Breusegem F (2002) Signal transduction during oxidative stress. *J Exp Bot* 53: 1227-1236. doi:10.1093/jexbot/53.372.1227. PubMed: 11997371.
36. Mittler R (2002) Oxidative stress, antioxidants and stress tolerance. *Trends Plant Sci* 7: 405-410. doi:10.1016/S1360-1385(02)02312-9. PubMed: 12234732.
37. Wise RR, Naylor AW (1987) Chilling-Enhanced Photooxidation : The Peroxidative Destruction of Lipids during Chilling Injury to Photosynthesis and Ultrastructure. *Plant Physiol* 83: 272-277. doi:10.1104/pp.83.2.272. PubMed: 16665235.
38. Waring P (2005) Redox active calcium ion channels and cell death. *Arch Biochem Biophys* 434: 33-42. doi:10.1016/j.abb.2004.08.001. PubMed: 15629106.
39. Yang T, Poovaiah BW (2002) Hydrogen peroxide homeostasis: activation of plant catalase by calcium/calmodulin. *Proc Natl Acad Sci U S A* 99: 4097-4102. doi:10.1073/pnas.052564899. PubMed: 11891305.
40. Traynelis SF, Wollmuth LP, McBain CJ, Menniti FS, Vance KM et al. (2010) Glutamate receptor ion channels: structure, regulation, and function. *Pharmacol Rev* 62: 405-496. doi:10.1124/pr.109.002451. PubMed: 20716669.
41. Knight H, Trewavas AJ, Knight MR (1996) Cold calcium signaling in *Arabidopsis* involves two cellular pools and a change in calcium signature after acclimation. *Plant Cell* 8: 489-503. doi:10.2307/3870327. PubMed: 8721751.
42. Kwaaitaal M, Huisman R, Maintz J, Reinstädler A, Panstruga R (2011) Ionotropic glutamate receptor (iGluR)-like channels mediate MAMP-induced calcium influx in *Arabidopsis thaliana*. *Biochem J* 440: 355-365. doi:10.1042/BJ20111112. PubMed: 21848515.
43. Knight MR, Campbell AK, Smith SM, Trewavas AJ (1991) Transgenic plant aequorin reports the effects of touch and cold-shock and elicitors on cytoplasmic calcium. *Nature* 352: 524-526. doi:10.1038/352524a0. PubMed: 1865907.